Roughening Transition of an Amorphous Metal Surface: A Molecular Dynamics Study

Pietro Ballone
Max-Planck Institut für Festkörperforschung, Heisenbergstrasse 1, 70569 Stuttgart, Germany

Silvia Rubini
Istituto Nazionale per la Fisica della Materia, Dipartimento di Fisica "A. Volta", Università di Pavia, Via Bassi 6, I-27100 Pavia, Italy

(Received 25 January 1996; revised manuscript received 6 May 1996)

By molecular dynamics with an embedded atom potential we study the surface properties of amorphous $Pd_{80}Si_{20}$. We analyze the evolution of structural and dynamical properties on cooling across the glass temperature T_g and we observe that the surface undergoes a deroughening transition 100 K below T_g, coincident with an anomaly in the surface diffusion. We show that the transition does not depend on the details of the interatomic potential, and appears to be a general consequence of the surface kinetics close to T_g. [S0031-9007(96)01376-2]

PACS numbers: 68.35.Bs, 61.43.Dq, 68.35.Rh, 68.45.Kg

Since amorphous metals are disordered and isotropic [1], one might think that their surfaces would be relatively simple, more akin to the liquid surface than to the crystal ones, with their variety of structures and phase transitions [2]. A closer look, however, suggests a number of intriguing questions, related to the crossover from liquidlike to solidlike behavior of structural, mechanical, and dynamical properties that has to take place around the glass transition. These questions add further interest to a subject of considerable importance because of the potential applications of amorphous metal surfaces in catalysis [3], and of their role in the kinetics of glass formation and recrystallization [4].

To gain insight into this subject, we perform molecular dynamics simulations for the surface of an amorphous metal alloy, i.e., $Pd_{80}Si_{20}$, based on the embedded atom method (EA [5]). On cooling slowly across the glass temperature T_g, we observe the evolution from a rough surface in the liquid to a smooth surface in the amorphous solid, taking place at a temperature T_R that is 100 K below T_g. This change appears to be a *bona fide* phase transition of order higher than first, displaying a close analogy with the roughening transition in crystal surfaces. To understand its origin, we analyze the evolution of the system properties around T_g. We observe that roughening coincides with an anomaly in the surface diffusion due to residual surface relaxation at a temperature T ($T < T_g$) for which the bulk is kinetically frozen. By contrast, the most apparent change in the surface dynamics close to T_g, i.e., the evolution from capillary waves in the liquid to phonons in the amorphous solid, takes place at a temperature higher than T_g, and cannot be directly related to roughening. We show that our results are insensitive to the details of the interatomic potential, and appear to be a general consequence of the system kinetics close to T_g.

Previous renormalization group computations [6] and Monte Carlo simulations [7] for lattice models of solid surfaces with quenched disorder and long range orientational order suggested the presence of a super-roughening transition at a temperature $T_{SR} < T_R$, below which the mean square fluctuation of the vertical position of the interface diverges faster than for a rough surface. Our simulation does not support this scenario for a truly amorphous system, and offers a different picture, at the same time less exotic than "super-roughening," but also very intriguing. As could be expected, the amorphous surface appears to be simply intermediate between the liquid and the solid surfaces, sharing features of both. On the other hand, the surface of amorphous metals is much less constrained by the bulk than crystal surfaces, and the admixture of liquid and solid features is different for the different properties that one considers. In particular, the continuous nature of the glass transition allows the changes in structural, dynamical, and thermodynamic properties to occur as independent transitions, while they would collapse at a single point in the case of a discontinuous first order transition like the freezing from liquid to crystalline solid.

Our computation is based on the EA potential for $Pd_{80}Si_{20}$ described in Ref. [8] and shown to reproduce the major features of $Pd_{80}Si_{20}$, without, however, achieving a fully quantitative description. The inaccuracies, discussed in Ref. [8], are compensated for by the simplicity of the model, which allows us to simulate large systems and long times with a workstation.

We simulate 22 112 Pd and 5536 Si atoms arranged on a slab of 48 Å width, limited by two square surfaces of side length $L = 96$ Å, perpendicular to the z axis and periodically repeated in the x-y plane. The slab is equilibrated during 50 ps at 1600 K, temperature well above the $T_g = 959$ K estimated for the model, and for which the atoms diffuse rapidly. The slab is quenched to 300 K by successive discontinuous rescaling of velocities. At each stage we decrease the temperature by 100 K, equilibrate the system for 16 ps, and perform a microcanonical

run of 16 ps to collect statistics. The total simulation covers more than 0.6 ns.

Preliminary results for a slab 4 times smaller, with the same surface to volume ratio, prepared with the same quenching rate have been reported in [9]. The static structure and thermodynamics computed for the two sizes are indistinguishable. In particular, the glass temperature is the same, and equal to the one computed in Ref. [8] for a bulk sample of 864 atoms periodic in three dimensions. Other results of the previous computation relevant to the present discussion can be summarized as follows: in the undercooled liquid range, from ~1800 K down to T_g, diffusion barriers are 700 K lower at the surface than in the bulk, resulting in an enhanced relaxation and ordering at the surface. The entire slab, however, is amorphous, and no crystal nucleus is formed during the simulation. This picture, confirmed by the present computation, is illustrated by the behavior of the density profile for Pd and Si as a function of z, reported in Fig. 1. The surface is enriched in Pd, but segregation does not extend more than 2 Å below the surface. Already at 1455 K, i.e., 400 K below the estimated melting point of the model, there is some tendency to layering in the Pd profile. Layering increases with decreasing T, and is clearly enhanced at the surface, but never approaches the degree of order characteristic of a crystal, however hot and defective [10]. The Si profile, on the other hand, does not display any significant ordering.

To discuss the surface structure, we need to identify the surface atoms. To this aim we attribute an atomic radius r_{Pd} and r_{Si} to Pd and Si [11], respectively, and we compute the area that each atom exposes to the free surface by Monte Carlo integration: we distribute random points on the surface, and we count how many of them fall within the disk associated to each atom. Points intercepted by more than one atom are attributed to the one with the highest (lowest) z for the upper (lower) surface. The area S_i exposed by atom i is computed as the ratio of the number N_i of intercepted points by the average density ρ_{RP} of random points: $S_i = N_i/\rho_{\mathrm{RP}}$. By using 10^5 random points we achieve an accuracy of a few percent in S_i. Finally, surface atoms are those exposing more than 30% of $\pi r^2_{\mathrm{Pd(Si)}}$ for Pd and Si, respectively. This definition reproduces the intuitive identification of surface atoms for the most common crystal surfaces; it is similar to those adopted in other studies [12], and is, to some extent, equally open to discussion. We verified, however, that the results are unaffected by small changes in the atomic radii, the number of random points, or the cutoff area used to define the surface atoms.

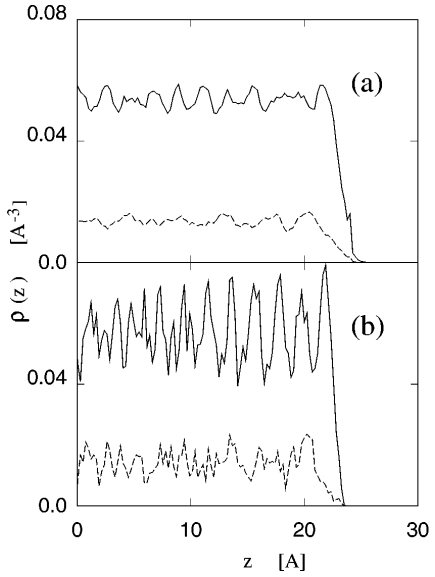

FIG. 1. Density profile averaged along the surface plane xy versus z in the undercooled liquid range at $T = 1455$ K (a), and at $T = 300$ K (b). Full line: Pd atoms, dashed line: Si atoms. Only half of the slab is displayed.

Surface roughness is usually discussed in terms of the height-height correlation function:

$$H(|\,\mathbf{R}_i - \mathbf{R}_j\,|) = \langle |\,h(\mathbf{R}_i) - h(\mathbf{R}_j)|^2 \rangle$$

where $h(R)$ is the vertical location of the surface at the (2D) position $\mathbf{R}$ in the surface plane. In our computation, for each configuration $h(\mathbf{R}_i)$ is defined by the z_i coordinate of the *surface atoms* whose position is $\{\mathbf{R}_i, z_i\}$. For a smooth surface $H(R)$ tends to a finite limit as $R \to \infty$, while, by definition, it diverges in the case of roughness. For liquid surfaces or rough surfaces on a crystal substrate, the divergence is logarithmic [2]. In the case of super-roughening [6], $H(R)$ is predicted to diverge as $\log^2(R)$. The $H(R)$ computed for our slab is displayed in Fig. 2 for the undercooled liquid range ($T = 1455$ K) and the amorphous phase ($T = 300$ K). In the first case, $H(R)$ has a clear logarithmic behavior. In the second case, $H(R)$ tends to a finite limit for $R \geq 35$ Å. At neither temperature the $\log^2(R)$ form characterizing super-roughening provides an accurate fit of the simulation.

Simulation studies of roughening are notoriously difficult because of the slow divergence of $H(R)$, requiring large systems and accurate statistics. The range for $\mathbf{R}$ reported in Fig. 2 ($12 < R < 40$ Å) has been selected in order to neglect the short range part, affected by large fluctuations, as well as the range beyond 40 Å (equal to 80% of $L/2$) that could be affected by finite size errors. To increase our confidence in the results, we include in Fig. 2 the points relative to the previous simulation with 6912 atoms, also cut at 12 Å and at 80% of $L/2$ (in this case 20 Å). The comparison underlines the good agreement of the two computations, and shows that a large system size ($R \geq 35$ Å) is required to distinguish the smooth from the rough behavior.

To characterize the transition in a quantitative way, for each simulated T we fit $H(R)$ by the superposition of the logarithmic component and a short range function:

$$H(R) = H_l \ln(R/R_c) + B \exp(-R/R_c) + C\,.$$

H_l, B, and C are free parameters, while $R_c = 8$ Å has been selected in order to have a short range part

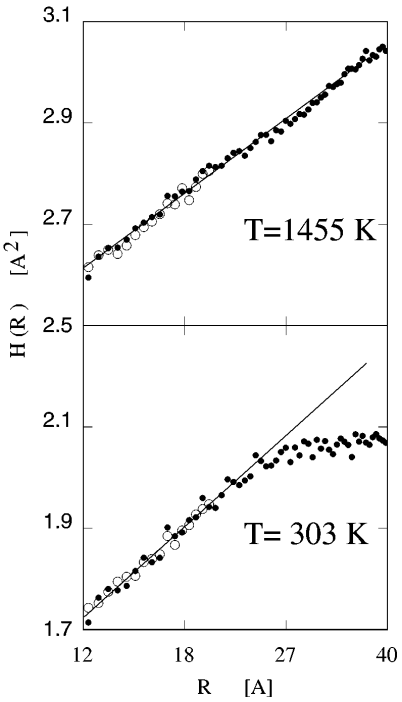

FIG. 2. Height-height correlation function H as a function of R. Dots: 27 648 atoms simulation; circles: 6912 atoms simulation. Note the logarithmic scale for R and the different vertical scales in the two plots. The full lines are the fit of the first half of the data with a $\ln(R)$ dependence.

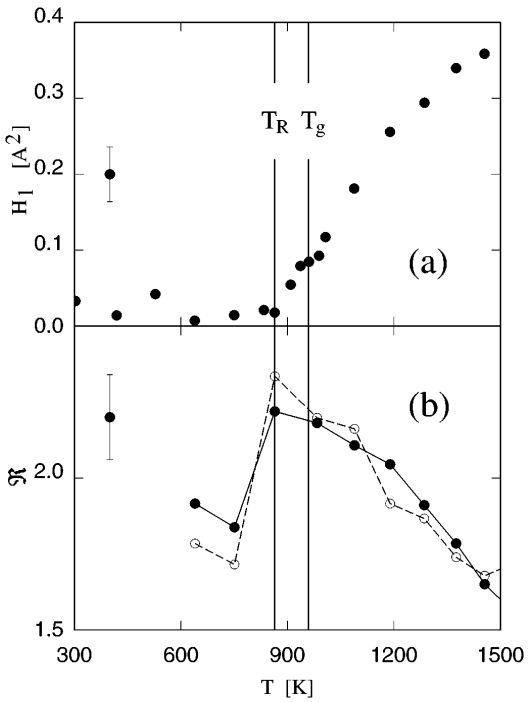

FIG. 3. (a) Amplitude H_l of the logarithmic part of H as a function of T (see text). (b) Ratio $\mathcal{R}$ of the diffusion coefficient for the "surface" atoms and the "bulk" atoms (see text). Full circles: Pd atoms; empty circles: Si atoms. Representative error bars are reported.

sufficiently linearly independent from the logarithm in the range $12 \leq R \leq 40$ Å. This form yields a remarkably accurate fit for $H(R)$. The plot for the amplitude H_l of the logarithmic part as a function of T (Fig. 3) allows us to locate the transition at $T_R = 850$ K, separating the rough phase at high T from the smooth one at low T, for which H_l is zero within the error bar. The figure suggests that H_l has the square root dependence on T ($H_l \sim \sqrt{T - T_R}$, $T \geq T_R$) characterizing the roughening of crystal surfaces. However, the error bars [estimated by dividing the statistics for $H(R)$ into two parts] do not allow a precise identification.

The roughening temperature T_R coincides with an anomaly in the surface diffusion observed in the previous study [9]. To investigate the relation of the two, we superimpose to Fig. 3 the ratio $\mathcal{R}$ of the diffusion coefficient for the surface atoms and for the atoms within the bulk (those located 10 Å away from the average surface plane). This plot confirms the picture proposed in the previous paper: surface relaxation is facilitated by low diffusion barriers, and enhances order at the surface. Particularly important is the discontinuity of $\mathcal{R}$ coincident with T_R, that was unexplained in the previous study. Our extended computation shows that the anomaly is real, and probably connected to the roughening transition: below T_R the restructuring of the surface increases the diffusion barriers and reduces the diffusion constant.

It would be tempting to relate the roughening transition to the transformation of the surface excitations from capillary waves in the liquid to phonons in the amorphous solid. To establish a connection with the continuum approximation inherent to the capillary wave picture, we define a continuous surface $Z(R, t)$ that, at each time t approximates the discrete atomistic surface. We express $Z(R, t)$ as a Fourier series:

$$Z(R, t) = \sum_q \{A_q(t) \cos(qR) + B_q(t) \sin(qR)\},$$

where $\mathbf{q}$ is a 2D wave vector compatible with the surface periodic boundary conditions. The sum is limited to $q \leq 0.7$ Å^{-1} (corresponding to ~150 terms) to define a function Z varying slowly in space. At each time t, $A_q(t)$ and $B_q(t)$ are computed by linear least squares fit to the instantaneous positions $z_i(\mathbf{R}_i, t)$ of the surface atoms. To isolate in $Z(\mathbf{R}, t)$ the dynamical excitations from static surface corrugations [that are described by $H(R)$], we subtract from $A_q(t)$ and $B_q(t)$ their time average, and we introduce the new variables $\bar{A}_q(t) = A_q(t) - \langle A_q(t) \rangle$ and $\bar{B}_q(t) = B_q(t) - \langle B_q(t) \rangle$ which describe the amplitude of the surface oscillations whose polarization is perpendicular to the surface plane. In Fig. 4 we report the average amplitude $W_q = \langle \sqrt{\bar{A}_q^2(t) + \bar{B}_q^2(t)} \rangle$ as a function of q for three temperatures. Capillary waves are characterized by $W_q \sim q^{-1}$ for low q [13], and we used this functional form to fit the simulation results. The fit is excellent for $T = 1455$ K, apart from a few points closest to $\mathbf{q} = 0$, affected by finite size effects, and supports the

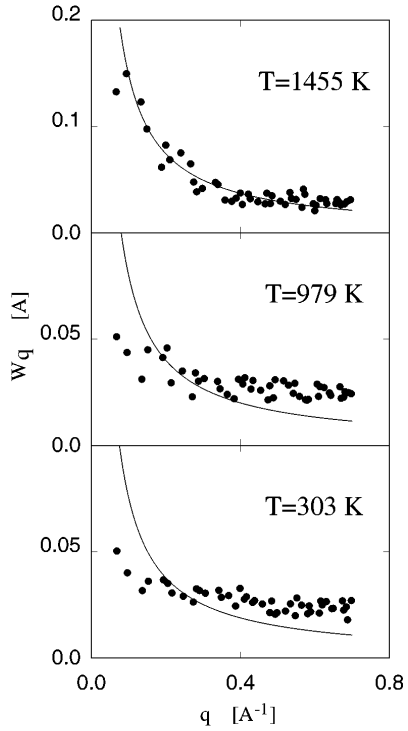

FIG. 4. Amplitude W_q of the surface excitations as a function of the modulus of the wave vector **q** (see text). Note the different scales. The full lines are fits of the data with αq^{-1}

description of the surface dynamics in terms of capillary waves. By contrast, the q^{-1} fit is apparently inadequate at the other two temperatures, including T_g. This shows that the transformation of the surface excitations from liquidlike to solidlike takes place at a temperature higher than T_g, and cannot be directly related to the roughening that occurs only 100 K below T_g.

To verify that our results are not an artifact of the short simulation time, we cycled the temperature over 500 K around T_g: we started ~200 K below T_g, increased T up to 1200 K, and decreased again to the starting T following the same procedure of the first quench. The properties computed in this short cycle reproduce those of the main computation well within the error bars.

Metals are characterized by many-body forces that compensate undercoordination at the surface by an increase of the atom-atom attraction. To evaluate the importance of this effect, which also tends to increase ordering at surfaces, we repeated our simulation with a pair potential that mimics as close as possible the properties of the bulk. In deriving the two-body potential from the EA one, we followed the prescription of Ref. [14]. This last computation shows that the results discussed above do not depend on the details of the potential: the glass temperature of the two-body model is only slightly lower than the EA one, the logarithmic amplitude H_l tends to be higher than that reported in Fig. 3 at high temperature, but also displays a clear roughening transition at a temperature T_R that is now 150 K below T_g.

To our knowledge, the most direct experimental information on the surface morphology of amorphous metals is provided by scanning tunneling microscopy images for $Rh_{25}Zr_{75}$ [15] and $Fe_{91}Zr_9$ [16], covering extended areas (~500 × 500 Å^2) at relatively low resolution. The images show large scales hills and grooves, as well as atomically flat terraces. Unfortunately, the aim of these studies being the catalytic applications of amorphous alloys, the conditions of the measurements were not optimized to highlight the intrinsic properties of the surface, and no systematic study of the surface structure as a function of temperature has been reported. The relation of those images with our simulation, therefore, is uncertain. It would be very interesting to image an amorphous metal surface at high resolution, and to test directly our simulation results by measuring the correlation function H for an area of ~100 × 100 Å^2. The surface should be aged at moderately high temperature (although safely below the recrystallization temperature) to obtain a reproducible structure. Under these conditions, the relatively wide temperature range of stability of roughness on amorphous substrates, and the fact that T_R and T_g are significantly lower than typical transition metal melting temperatures, could provide a suitable testing ground for the statistical mechanics and thermodynamics of the roughening transition.

We thank M. Bernasconi, W. Kress and M. Parrinello for useful discussions.

[1] *Glassy Metals*, edited by H. Beck and H.-J. Güntherodt (Springer, Heidelberg, 1994), Vol. III.
[2] A. Zangwill, *Physics at Surfaces* (Cambridge University Press, Cambridge, 1988); M. Bernasconi and E. Tosatti, Surf. Sci. Rep. **17**, 363 (1993).
[3] G. V. Smith *et al.*, in *Proceedings of the 7th International Congress on Catalysis*, edited by T. Seiyama and K. Tanabe (Elsevier, New York, 1981), Vol. A.
[4] A. Calka and A. P. Radinski, Mater. Res. Soc. Symp. Proc. **80**, 195 (1987); U. Köster and B. Punge-Wittler, Mater. Res. Soc. Symp. Proc. **80**, 355 (1987).
[5] M. S. Daw and M. I. Baskes, Phys. Rev. Lett. **50**, 1285 (1983); Phys. Rev. B **29**, 6443 (1984).
[6] J. Toner and D. P. DiVincenzo, Phys. Rev. B **41**, 632 (1990); S. Scheidl, Phys. Rev. Lett. **75**, 4760 (1995).
[7] D. Cule and Y. Shapir, Phys. Rev. Lett. **74**, 114 (1995).
[8] P. Ballone and S. Rubini, Phys. Rev. B **51**, 14 962 (1995).
[9] P. Ballone and S. Rubini, Surf. Sci. **342**, L1116 (1995).
[10] J. Q. Broughton and G. H. Gillmer, J. Chem. Phys. **79**, 5105 (1983).
[11] The radius is equal to one-half of the nearest neighbor distance in the crystal structure used to gauge the potential for Pd and Si.: $r_{Pd} = 1.38$ Å, $r_{Si} = 1.27$ Å.
[12] S. Iarlori *et al.*, Surf. Sci. **211/212**, 55 (1989).
[13] C. A. Croxton, *Statistical Mechanics of the Liquid Surface* (Wiley, Chichester, 1980).
[14] S. M. Foiles, Phys. Rev. B **32**, 3409 (1985).
[15] R. Wiesendanger *et al.*, Surf. Sci. **181**, 46 (1987).
[16] B. Walz *et al.*, Mater. Sci. Eng. **99**, 501 (1988); R. Schlögl, R. Wiesendanger, and A. Baiker, J. Catal. **108**, 452 (1987).